Comparative Lifetime Estimations for IGBT Modules in Wind Turbine Converters

Christian Neumann, Hans-Günter Eckel
UNIVERSITY OF ROSTOCK
Albert-Einstein-Str. 2
D-18059 Rostock, Germany
Tel.: +49 381 / 498-7138
E-Mail: christian.neumann@uni-rostock.de
URL: http://www.iee.uni-rostock.de/

Acknowledgements

The project WindVolt (0324256B) is supported by the Federal Ministry for Economic Affairs and Energy on the basis of a decision by the German Bundestag.

Keywords

«IGBT», «Lifetime», «Reliability», «Thermal cycling», «Wind energy».

Abstract

Comparative IGBT lifetime estimations for a generic wind turbine are presented. A thermal impedance matrix is utilized for thermal modeling, addressing thermal cross-coupling effects within the IGBT modules. For the estimation procedure, all temperature swings are calculated with a high temporal resolution, allowing the correct superposition of each swing.

Introduction

The overall thermal stress for IGBT modules in wind power applications consists of a superposition of fundamental frequency cycles correlated to the converter's output frequency and low-frequency cycles, caused by changing operation points due to fluctuations in wind speed [1]. Thus, the resulting mission profiles are complex, and it is mandatory to consider them as accurately as possible for realistic lifetime estimation.
The lifetime estimation procedures typically perform calculations on different time frames and merge the identified life consumptions to an overall result [2]. A lower time resolution is chosen to deal with wind-induced load changes, which results in averaged temperature profiles. Furthermore, it neglects the fundamental frequency ripple on top of them, as this is not displayed in the considered time frame. Consequently, the estimation procedures will operate on trivialized loading conditions, which do not represent the realistic stress an IGBT module has to endure. The lower the fundamental frequency of the converters, the higher this issue becomes. Moreover, the thermal model of the converter is often described as a Y-model [3]. This only addresses thermal cross-coupling effects between the IGBTs and *Free-Wheeling Diodes* (FWDs) on the case or heatsink level, but they already appear on the substrate level due to lateral heat spreading [4]. Both points mentioned above will lead to an overestimated lifetime of the IGBT modules.

This paper presents a lifetime estimation procedure that tackles the mentioned issues. The necessary calculations of the semiconductor losses and temperatures are performed on a high-resolution time basis. Hence, the mission profiles as inputs are transferred into temperature profiles, which contain thermal cycles from operation point changes and fundamental frequency components. Moreover, utilizing a thermal impedance matrix instead of a Y-model considers thermal cross-coupling effects way earlier. Hence, the loading conditions for the IGBT modules are mapped more realistically.
The investigations are carried out for the IGBT modules in the *Machine-Side Converter* (MSC) of a generic full-scale converter wind turbine (type 4) in the 3 MW class. Fig.1 illustrates the lifetime estimation procedure, which takes place in three steps.

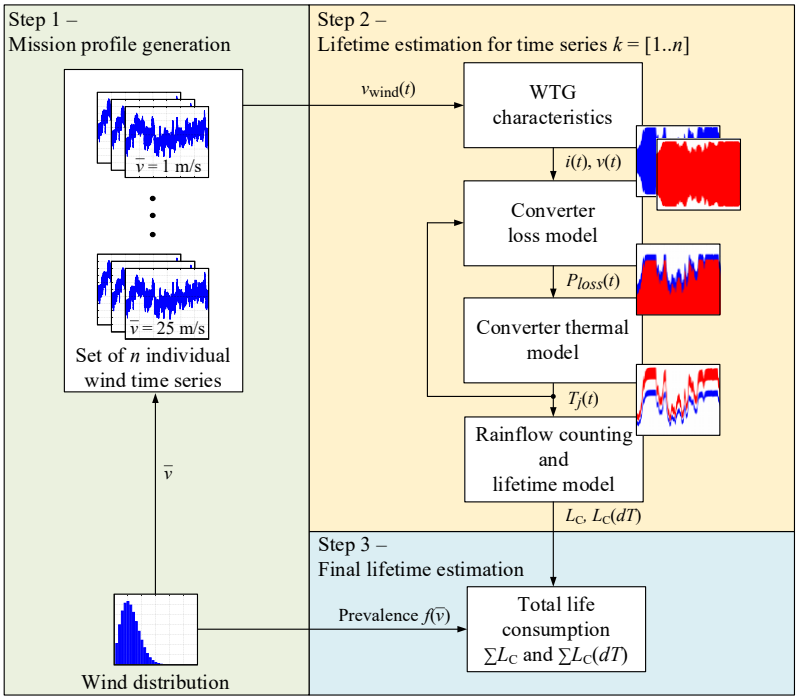

Fig. 1: Lifetime estimation procedure

A set of n synthetic wind time series at various average wind speeds will represent the mission profiles. They are used to calculate the thermal cyclings $T_j(t)$ of IGBTs and FWDs based on the converter's power losses and thermal models. A rainflow counting algorithm [5] is used to evaluate the thermal cyclings of the individual wind time series k regarding their height and quantity. By applying those thermal cycles to the lifetime model of the manufacturer and considering Miner's rule for damage accumulation, the relative life consumption (L_c) of the k^{th} wind time series can be estimated. However, thermal cycles below 10 K are assumed to cause no harm to the module. Based on the prevalence of each average wind speed, which is defined by a Rayleigh wind distribution, those individual life consumptions are accumulated to an overall result ($\sum L_c$) . The targeted lifetime in this paper is 20 years.
The converters for the comparative study are equipped with 1700 V half-bridge IGBT modules from Infineon. The upper IGBT and FWD are referred to as I_1 and D_1, whereas I_2 and D_2 is used for the lower ones. As the losses and thermal models for the upper and lower IGBT / FWD are identical, only the results for I_1 and D_1 are presented in this paper. Usually, a parallel connection of N IGBT modules is used for the converters. An equal current distribution among the paralleled modules is assumed, so the collector current I_C of a single IGBT or FWD shares $1/N$ of the total MSC current. As the main focus of the generic approach is to identify and investigate influencing factors on the estimated lifetime, the number of paralleled modules N does not necessarily have to be an integer value – quite contrary to real applications. Instead, N is set to meet a defined $T_{j,max}$ of the switches during operation at nominal power.

The generic approach allows the investigation of several influencing factors on the estimated lifetime. This paper covers different design and modeling aspects, like the thermal utilization of the IGBT modules or the base frequency of the generator, and the influence of the input's temporal resolution.

General model description

The following subsections explain the essential parts of the lifetime estimation procedure in more detail.

Wind profiles and wind distribution

In this study, 10-minutes stochastic wind time series are generated according to IEC 61400-3 using the Kaimal *Power Spectral Density* (PSD) to model wind turbulence [6]. The PSD is calculated for several mean wind speeds $\bar{v}_{hub}$ on the wind turbine's hub height (1). A Rayleigh distribution, with a wind site-specific mean wind speed $\bar{v}$, states the prevalence for $\bar{v}_{hub}$ over one year in bars of 1 m/s (2).

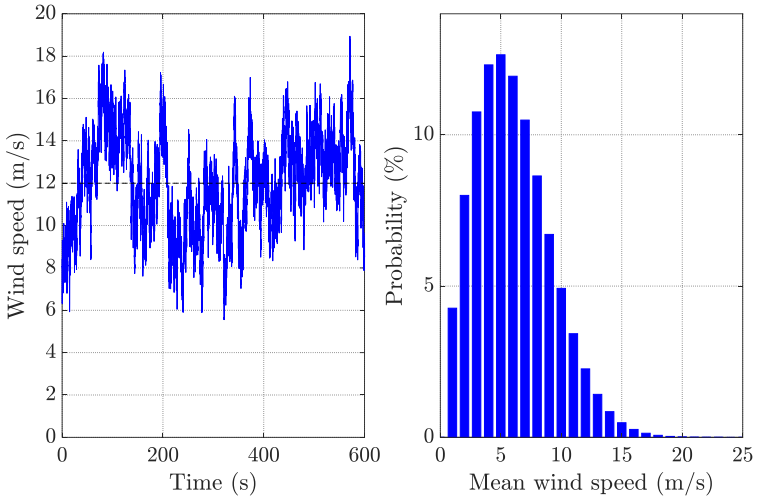

Fig. 2: Wind time series with a mean wind speed of 12 m/s (left); Rayleigh distribution for a wind site with an average wind speed of 6 m/s (right)

$$S_{\mathrm{k}}(f) = 4\sigma_{\mathrm{k}}^2 \frac{\frac{L_{\mathrm{k}}}{\bar{v}_{\mathrm{hub}}}}{\left(1 + 6f\frac{L_{\mathrm{k}}}{\bar{v}_{\mathrm{hub}}}\right)^{\frac{5}{3}}} \tag{1}$$

$$f(v) = \frac{\pi v}{2\bar{v}^2} \mathrm{e}^{-0.25\pi(v/\bar{v})^2} \tag{2}$$

In the equations, $L_{\mathrm{k}} = 340.2$ m denotes a turbulence length scale parameter for hub heights above 60 m [6] and σ_{k} is the standard deviation of the wind turbulence determined by the *Turbulence Intensity* (TI). The lifetime estimation is consecutively performed for all n wind time series. This study has two individual wind time series for each mean wind speed between 1 m/s and 25 m/s ($n = 50$).
Fig. 2 shows an exemplary wind time series for IEC class A, represented by a TI of 18%, and a Rayleigh distribution for an IEC class III wind site, having less than 7.5 m/s average wind speed on hub height.

Generator and MSC control structures

A *Permanent Magnet Synchronous Generator* (PMSG) is utilized for the type 4 wind turbine concept. The generator and converters are modeled with characteristic curves and equations to simulate their quasi-stationary behavior. At this calculation stage, an interpolation of the k^{th} input wind time series to a higher time resolution is performed, which is chosen to represent the expected fundamental frequency cycles properly. Relations between the input wind speed, generator speed, and generator torque can be derived from the generic wind turbine's characteristics, shown in Fig. 3. However, the wind speed can not be directly translated into the generator quantities, as the dynamics would be way too fast. Instead, the wind speed is filtered by a first-order lowpass filter with the turbine's inertia constant $H = 4$ s to respect the mechanical dynamics of the drivetrain.

The mechanical generator quantities are transferred into the instantaneous MSC electrical quantities by using the necessary equations for the PMSG (3)-(5) and assuming an MSC *Field Oriented Control* (FOC) with *Zero d-axis Current* (ZDC) control strategy [7].

$$v_{\mathrm{sd}} = R_{\mathrm{sd}} i_{\mathrm{sd}} + L_{\mathrm{sd}} \frac{di_{\mathrm{sd}}}{dt} - \omega_{\mathrm{e}} L_{\mathrm{sq}} i_{\mathrm{sq}} \tag{3}$$

$$v_{\mathrm{sq}} = R_{\mathrm{sq}} i_{\mathrm{sq}} + L_{\mathrm{sq}} \frac{di_{\mathrm{sq}}}{dt} + \omega_{\mathrm{e}} L_{\mathrm{sd}} i_{\mathrm{sd}} + \omega_{\mathrm{e}} \psi_{\mathrm{m}} \tag{4}$$

$$T_{\mathrm{e}} = \frac{3p}{2} (\psi_{\mathrm{m}} i_{\mathrm{sq}} - (L_{\mathrm{sd}} - L_{\mathrm{sq}}) i_{\mathrm{sd}} i_{\mathrm{sq}}) \tag{5}$$

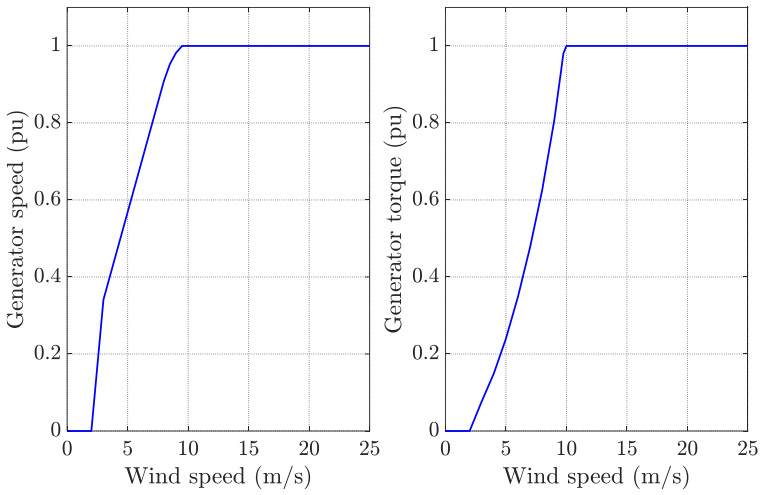

Fig. 3: Characteristic curves for generator speed (left) and torque (right) of the generic wind turbine

Based on the generator torque gathered from the characteristics (see Fig. 3) in combination with the input wind speed, dq-phasors for current and voltage of the MSC can be calculated. Hence, the instantaneous MSC currents and voltages can be derived, as shown for phase a, when the d-axis is chosen as phasor reference.

$$i_a(t) = i_{sq}\sin(\omega_e t - \frac{\pi}{2}) \tag{6}$$

$$v_a(t) = \sqrt{v_{sd}^2 + v_{sq}^2}\sin(\omega_e t + \varphi_v) \tag{7}$$

Where φ_v denotes the angle of the dq-voltage phasor regarding the d-axis.

Power loss and thermal model

The calculation of conduction and switching losses is based on datasheet values of the investigated IGBT modules. A curve-fitting approach is utilized to find the corresponding data regarding currents and junction temperatures T_j for different operation points, and instantaneous power losses are calculated for the upper and lower IGBT / FWD. The switching losses are determined by the junction temperature T_j, collector current I_C, DC voltage V_{dc}, and switching frequency f_{sw}. The conduction losses are defined as a function of T_j, I_C, and the relative duty cycle τ. A Pulse-Width Modulation (PWM) with a third harmonic injection is assumed for the latter one.

Because half-bridge IGBT modules are used, thermal cross-couplings between the upper and lower switches have to be considered in the lifetime estimation [4]. A matrix approach for thermal modeling is used to address this issue. All transient thermal impedances in (8) are given from junction to ambient and describe the thermal transfer between two nodes, e.g., the portion of passive heating seen at I_1 while D_1 is producing power losses (see $Z_{th,ja\ D_1I_1}$).

$$\begin{bmatrix} T_{j\,I1} \\ T_{j\,D1} \\ T_{j\,I2} \\ T_{j\,D2} \end{bmatrix} = \begin{bmatrix} Z_{th,ja\,I1I1} & Z_{th,ja\,D1I1} & Z_{th,ja\,I2I1} & Z_{th,ja\,D2I1} \\ Z_{th,ja\,I1D1} & Z_{th,ja\,D1D1} & Z_{th,ja\,I2D1} & Z_{th,ja\,D2D1} \\ Z_{th,ja\,I1I2} & Z_{th,ja\,D1I2} & Z_{th,ja\,I2I2} & Z_{th,ja\,D2I2} \\ Z_{th,ja\,I1D2} & Z_{th,ja\,D1D2} & Z_{th,ja\,I2D2} & Z_{th,ja\,D2D2} \end{bmatrix} \begin{bmatrix} P_{I1} \\ P_{D1} \\ P_{I2} \\ P_{D2} \end{bmatrix} + T_a \tag{8}$$

The thermal impedances of the IGBT modules ($Z_{th,jc}$) and the generic heatsink ($Z_{th,ca}$) are given for Foster-type equivalent networks. Before connecting them in series, they have to be transformed into Cauer networks first. Cauer-type equivalent networks have a physical meaning and can be used for constructing a complete thermal system [8]. The resulting thermal impedances ($Z_{th,ja}$) are validated against real-world data. The junction temperatures can be estimated by calculating (8) with the instantaneous power losses. They contain ripples from changes in the wind conditions and the fundamental frequency component. A constant ambient temperature $T_a = 40$ °C is used in this case study.

Rainflow counting, lifetime model, and lifetime estimation

The derived junction temperatures of the k^{th} wind time series are further processed to a rainflow counting algorithm, which analyzes the thermal cycles regarding their cycle height, duration, number, and maximum junction temperature at which those cycles occur [5]. The results are applied to the lifetime model, which is not given in the form of an analytical function but the supplier's power cycling capability diagrams. The diagrams used here account for bond wire failures or wear out of the chip solder joints and represent the B_5 lifetime of the IGBT modules [9]. With this, the relative life consumption of the k^{th} wind time series can be estimated by opposing the actual cycles against the cycles to failure from the curves. Finally, the individual results for all n calculations are accumulated using the prevalence of each average wind speed given by the wind distribution.
The following example might help for a better understanding of the procedure. Assuming $k = 9$ and $k = 10$ represent both the 10-minutes wind time series with a mean wind speed of 5 m/s, resulting in a relative life consumption of 3e-7 (pu) and 5e-7 (pu), respectively. Furthermore, the average wind speed of 5 m/s shall have a yearly prevalence of 12%. Hence, 126144 of these 10-minutes cycles will be seen over 20 years. The share of the overall life consumption is calculated to:

$$\sum L_c(5\ \text{m/s}) = \frac{126144}{2}\,(3\text{e-}7 + 5\text{e-}7) = 0.1\ (\text{pu}) \tag{9}$$

Meaning these 5 m/s wind bins will consume 10% of the 20-years lifetime.

Besides showing absolute numbers, cumulative life consumption plots are used for visualizing the results. They indicate which percentage of the 20-years lifetime is consumed for cycles up to a certain dT. Moreover, they show which dT has the highest contribution to overall life consumption (see Fig. 4).

Case studies with influencing factors on the estimated lifetime

This section presents various lifetime estimation results for the MSC IGBT modules according to the influencing factors mentioned in the beginning. A base case scenario is defined to establish a reference for the following comparison:

- Weak wind location with an average wind speed of 6 m/s on hub height (IEC IIIA, TI = 18%)
- Wind time series with a temporal resolution of 0.018 s
- Infineon 4th generation IGBT modules with 1400 A nominal current (FF1400R17IP4)
- Thermal design $T_{j,max}$ = 125 °C resulting in N = 3.9 parallel IGBT modules
- High-speed PMSG with 50 Hz fundamental frequency at nominal speed

First of all, a lifetime estimation for the base scenario is performed. Fig. 4 shows the cumulative life consumption as a function of the cycle height dT for the IGBT and FWD. On the one hand, this form of the presentation shows the overall life consumption on a 20 years basis, where any value higher than one results in a lifetime of fewer than 20 years. On the other hand, it also reveals which share of the overall life consumption different cycle heights will cause.
As expected, the FWD is the lifetime limiting factor on the MSC due to the rectifier operation of the converter. The life consumption of the FWD sums up to 275%, representing an estimated lifetime of only seven years. However, the IGBT reaches 28% or 71 years, respectively. Additionally, two regions can be identified on the FWD curve that show a significant share of life consumption. The first step can be seen in lower thermal cycles around 12 K. These cycles have their origin in the fundamental frequency of the converter output currents. In this example, they consume about 13% of the 20-year lifetime. Higher cycles arise from changes in the wind turbine operation points induced by fluctuating wind speeds. They result in a much higher life consumption of roughly 260 %, and hence it is crucial to consider them in lifetime estimation procedures in any case. By only investigating the fundamental frequency cycles of the IGBT module, based on the prevalences of the operation points, the potential lifetime issue would not have been identified in this case.

The following sub-sections present detailed lifetime estimation results for selected influencing factors. Table I gives a complete overview of all simulated aspects within this work.

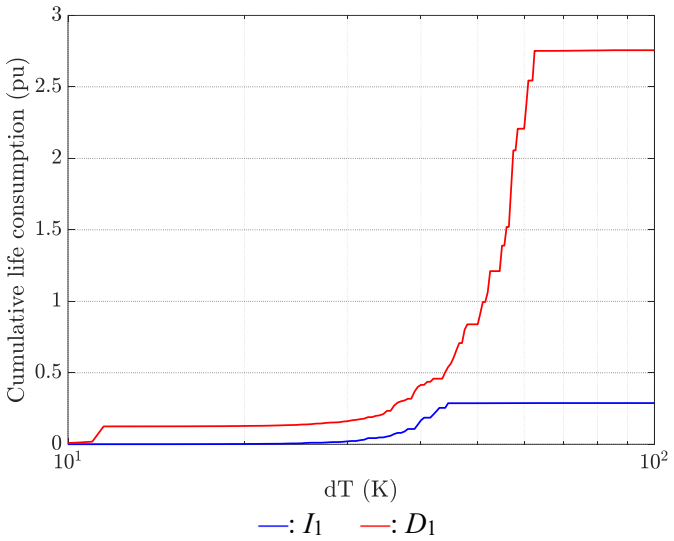

Fig. 4: Cumulative life consumption of the MSC IGBT modules for the base scenario

The thermal utilization level of the IGBT modules

The manufacturer's power cycling curves reveal higher $T_{j,max}$ results in fewer allowed cycles for the same thermal cycle height dT until the IGBT module might fail [9]. Hence, the thermal design temperature severely influences the estimated lifetime as cycles happening at higher maximum junction temperatures will lead to a higher life consumption and vice versa. Therefore, a comparative MSC design with a maximum junction temperature of 100 °C is utilized. In contrast to the base case, 5.83 instead of 3.9 modules are used in parallel to achieve lower junction temperatures on the devices.
Fig. 5 shows the cumulative life consumption curves for both cases. The increased number of IGBT modules results in lower losses on the individual IGBT module and smaller thermal cycles dT overall. Moreover, these cycles will happen at lower maximum junction temperatures, so the estimated lifetime is immensely increased from approximately seven to 76 years. Fundamental frequency cycles now occur below 10 K and do not cause any life consumption on the IGBT module as per the initial assumption.

The fundamental frequency of the converter

A notably challenging condition for the MSC IGBT modules arises with low-speed generator systems. In this case, the fundamental frequency of the converter's output currents is relatively low, resulting in

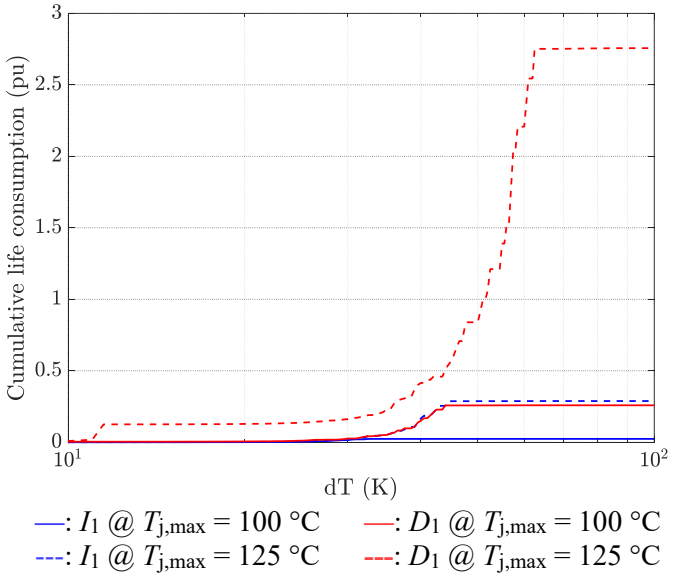

Fig. 5: Cumulative life consumption of the MSC IGBT modules for different thermal design $T_{j,max}$

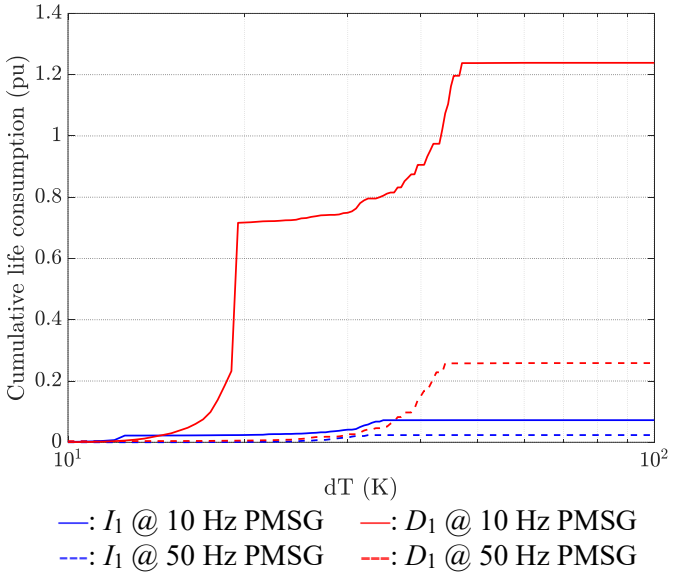

Fig. 6: Cumulative life consumption of the MSC IGBT modules for different fundamental frequencies of the PMSG and reduced $T_{j,max}$ = 100 °C

extended heating periods for the power semiconductors and higher thermal cycles dT in general [1]. This sub-section compares a 50 Hz indirect-driven and a 10 Hz direct-driven PMSG. As the base scenario with a high-speed generator was already not fulfilling the lifetime requirements of 20 years, the estimated lifetime on a low-speed generator will be even lower. Therefore, the comparison in Fig. 6 will be shown for the variant with an already reduced maximum junction temperature $T_{j,max}$ = 100 °C from the previous sub-section.

Fig. 6 shows a significant step in the cumulative life consumption for cycles up to 20 K, representing the fundamental frequency cycles for the low-speed generator case. Due to the increased cycle height, 72 % of the lifetime is consumed already. With the mission profile-based cycles included, a life consumption of 124% is calculated, resulting in an estimated lifetime of only 16 years. The target lifetime could not be met even though 100 °C is a cautious design temperature for the IGBT modules.

The temporal resolution of the input wind time series

As highlighted in the beginning, a lower temporal resolution or averaged wind speeds are often used in lifetime estimation procedures to deal with wind-induced load changes [2]. The original wind time series inputs, having a temporal resolution of 0.018 s, are averaged in 10 s and one-minute intervals to replicate this effect.

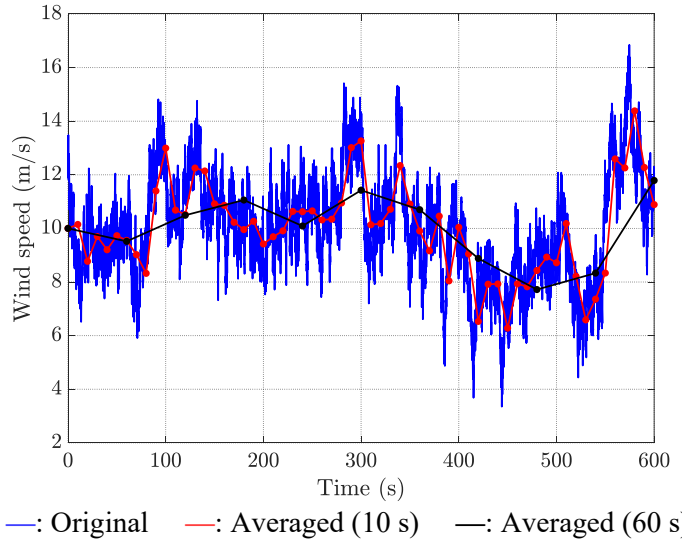

Fig. 7: Wind time series with a mean wind speed of 10 m/s (TI = 18%) with and without averaging

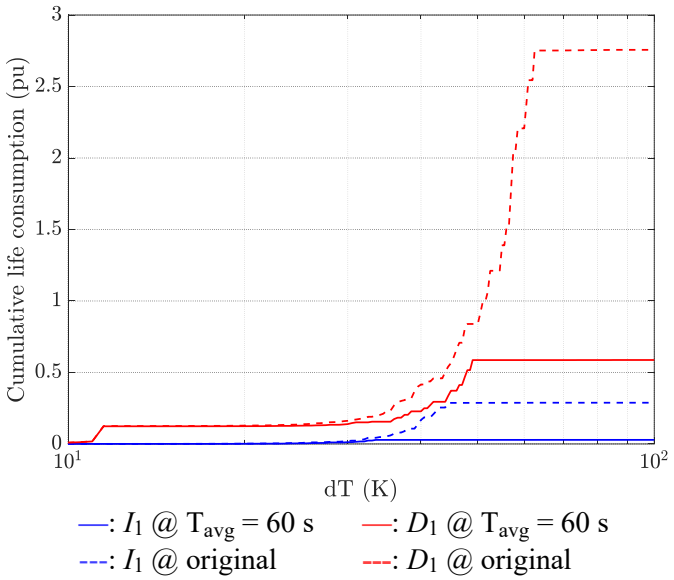

Fig. 8: Cumulative life consumption of the MSC IGBT modules for 60 s averaged and non averaged wind time series inputs

Fig. 7 shows an exemplary wind time series with a mean wind speed of 10 m/s. A short-term averaging removes the turbulence from the signal, which has quite the same effect as the filtering with the inertia constant H. However, the local peaks and dips are minimized the more prolonged the averaging period becomes. Hence, averaging the wind data results in understated load scenarios for the semiconductors, which will affect the lifetime estimation results - especially for the partial load cases where more operation point changes are about to happen due to changes in wind speed.
Fig. 8 compares the one-minute averaging to the base scenario. The fundamental frequency cycles of the diode show the same life consumption in both cases, which was to be expected. Still, a significant difference can be seen in the wind-induced cycles in higher dT regions. On the one hand, the maximum cycle height of the lifetime relevant cycles is reduced. On the other hand, lesser wind-induced cycles are occurring due to the averaging, which results in a lower life consumption and can be seen in the separation of both FWD curves starting at 20 K cycles. The estimated lifetime has increased from seven to over 34 years. However, the averaging with 10 s has not changed the estimated lifetime as the averaging and filtering effect is quite similar (see Table I).

Other influencing factors

Table I shows the results of all lifetime estimations performed on the MSC. The colors indicate how well the targeted lifetime of 20 years is achieved – not reached (red), attained but with a low margin (orange), or entirely accomplished (green).
Besides the points highlighted in the previous sub-sections, variations in the wind conditions were conducted. Three different locations, represented by their annual mean wind speeds, are assumed for the same wind turbine with a nominal wind speed of 10 m/s. Sites with a lower mean wind speed will increase the amount of partial load operation points, where thermal cycles are generally happening at lower maximum junction temperatures. Therefore, the estimated lifetime increases with lower mean wind speeds. Interestingly, the portion of the relative life consumption caused by wind-induced cycles strongly increases when the mean wind speed of the site approaches the steep part of the wind turbine's power curve because changes from partial to full load are about to happen more frequently. In this case, many thermal cycles from lower temperatures to the designed maximum junction temperature will be seen, leading to a higher life consumption. Fig. 9 illustrates the described effects showing the three Rayleigh distributions against the wind turbine's power curve and the corresponding life consumption curves for the FWD D_1.
Furthermore, a wind class B with a lower turbulence intensity than class A is considered. The reduced turbulence in the wind data also reduces the wind-induced cycles and positively affects the estimated lifetime in all cases.

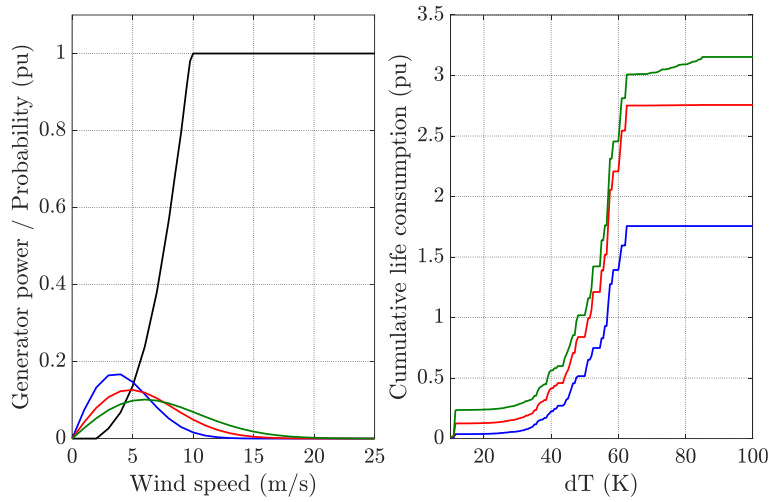

Fig. 9: Power curve versus Rayleigh distributions for three different locations (left); Cumulative life consumption of the MSC IGBT modules (D_1) for FF1400R17IP4 with designed $T_{j,max}$ = 125 °C (right)

Finally, different generations of the power modules are considered. In [10], the superior power cycling capability of Infineon's 5th generation power modules (FF1800R17IP5) over the 4th generation is shown. For the same maximum junction temperature, the estimated lifetime is much higher in all cases. Even for the challenging low-speed PMSG with $T_{j,max}$ = 125 °C, the estimated lifetime is close to or above the targeted value. The main reason, in this case, is the much higher power cycling capability for the fundamental frequency cycles.

Table I: Results of the MSC lifetime estimation

PMSG	**High-speed PMSG (50 Hz)**				**Low-speed PMSG (10 Hz)**			
IGBT modules	IGBT4 FF1400R17IP4		IGBT5 FF1800R17IP5		IGBT4 FF1400R17IP4		IGBT5 FF1800R17IP5	
$T_{j,max}$ / **Wind class**	100 °C N = 5.83	125 °C N = 3.9	100 °C N = 5.62	125 °C N = 3.7	100 °C N = 6.89	125 °C N = 4.56	100 °C N = 6.5	125 °C N = 4.22
IEC IIIA 4.5 m/s	113 (0 %)	11 (4 %)	544 (0 %)	69 (0 %)	33 (24 %)	2 (442 %)	279 (0 %)	34 (3 %)
IEC IIIA 6.0 m/s	77 (0 %)	7 (13 %)	400 (0 %)	48 (0 %)	16 (72 %)	1 (1350 %)	195 (1 %)	23 (9 %)
IEC IIIA 6.0 m/s (10 s avg.)	-	7 (13 %)	-	-	16 (72 %)	-	-	-
IEC IIIA 6.0 m/s (60 s avg.)	934 (0 %)	34 (12 %)	>1000 (0 %)	524 (0 %)	26 (67 %)	1 (1270 %)	936 (1 %)	103 (8 %)
IEC IIIB 6.0 m/s (TI = 16%)	220 (0 %)	14 (12 %)	>1000 (0 %)	129 (0 %)	20 (70 %)	1 (1320 %)	389 (1 %)	44 (8 %)
IEC IIIA 7.5 m/s	68 (0 %)	6 (24 %)	367 (0 %)	43 (0 %)	10 (125 %)	<1 (2400 %)	176 (2 %)	20 (14 %)

The table shows the estimated lifetimes in years, limited by the diodes of the MSC. Cases marked with "-" were not considered. The explanation for the base-case scenario with 7 (13 %): The relative life consumption on a 20-year basis is 275 %, leading to a round-off lifetime of 7 years. Only 13 % of the 20-years lifetime was consumed by the fundamental frequency and 264 % by wind-induced cycles.

Conclusion

This paper presents an IGBT module lifetime estimation procedure based on synthetic wind time series inputs and a generic type 4 wind turbine. The parameters used in this paper are matched against real-world data for wind turbines, generators, and wind turbine converters.
The approach considers the superposition of fundamental frequency and wind-induced thermal cycles,

as it performs necessary calculations with a high temporal resolution. Hence, it differs from known lifetime estimation procedures, which usually indicate no lifetime issues in their case studies [2]-[3]. However, there is still ongoing work to answer how these superimposed thermal cycles affect the IGBT module's lifetime, which is not part of typical power cycling tests. Additional research with the testbench introduced in [11] might help answer this question and validate the proposed method.
The generic approach allows for case studies with comparisons for controlled changes of the inputs to investigate various influencing factors on the estimated lifetime. This comparative MSC analysis might help to identify potential IGBT lifetime issues in real applications if certain conditions are fulfilled.

Parameters

Table II: Parameters of the generic wind turbine and PMSG

Parameter	Symbol (Unit)	High-speed version	Low-speed version
Wind turbine			
Rated power	S (MVA) / P (MW)	3.3 / 3.0	
Hub height	h_{hub} (m)	140	
Rotor diameter	d_{R} (m)	126	
Inertia constant H	H (s)	4	
Nominal rotor speed	n_{R} (rpm)	10	
Nominal wind speed	v_{R} (m/s)	10	
Wind speed operation range	v_{min} (m/s) / v_{max} (m/s)	3 / 25	
Gearbox ratio	i	1:100	-
PMSG			
Nominal voltage	V_{n} (V)	710	
Back EMF at nominal speed	V_{p} (V)	373	
Nominal speed	n_{G} (rpm)	1000	10
Number of pole pairs	p	3	60
Permanent flux	Ψ_{m} (Vs)	1.19	5.94
Inductances in d- and q- axis	L_{d} / L_{q} (mH)	0.145 / 0.200	0.745 / 1.0

Table III: Foster thermal impedance parameters of the generic heatsink

i / Z_{th}	1		2		3		4	
	R_{th} (K/kW)	τ (s)	R_{th} (K/kW)	τ (s)	R_{th} (K/kW)	τ (s)	R_{th} (K/kW)	τ (s)
$Z_{\mathrm{th,ja}}$ *I1I1*	0.2	0.004	4.62	0.695	3.54	1.046	21.84	6.107
$Z_{\mathrm{th,ja}}$ *D1I1*	0.15	0.004	3.465	0.695	2.655	1.046	16.38	6.107
$Z_{\mathrm{th,ja}}$ *I2I1*	0.078	0.008	1.797	1.39	1.377	2.092	8.493	12.214
$Z_{\mathrm{th,ja}}$ *D2I1*	0.1	0.008	2.31	1.39	1.77	2.092	10.92	12.214
$Z_{\mathrm{th,ja}}$ *I1D1*	0.117	0.004	2.695	0.695	2.065	1.046	12.74	6.107
$Z_{\mathrm{th,ja}}$ *D1D1*	0.317	0.004	7.315	0.695	5.605	1.046	34.58	6.107
$Z_{\mathrm{th,ja}}$ *I2D1*	0.078	0.008	1.797	1.39	1.377	2.092	8.493	12.214
$Z_{\mathrm{th,ja}}$ *D2D1*	0.1	0.008	2.31	1.39	1.77	2.092	10.92	12.214
$Z_{\mathrm{th,ja}}$ *I1I2*	0.078	0.008	1.797	1.39	1.377	2.092	8.493	12.214
$Z_{\mathrm{th,ja}}$ *D1I2*	0.1	0.008	2.31	1.39	1.77	2.092	10.92	12.214
$Z_{\mathrm{th,ja}}$ *I2I2*	0.2	0.004	4.62	0.695	3.54	1.046	21.84	6.107
$Z_{\mathrm{th,ja}}$ *D2I2*	0.15	0.004	3.465	0.695	2.655	1.046	16.38	6.107
$Z_{\mathrm{th,ja}}$ *I1D2*	0.078	0.008	1.797	1.39	1.377	2.092	8.493	12.214
$Z_{\mathrm{th,ja}}$ *D1D2*	0.1	0.008	2.31	1.39	1.77	2.092	10.92	12.214
$Z_{\mathrm{th,ja}}$ *I2D2*	0.117	0.004	2.695	0.695	2.065	1.046	12.74	6.107
$Z_{\mathrm{th,ja}}$ *D2D2*	0.317	0.004	7.315	0.695	5.605	1.046	34.58	6.107

References

[1] D. Weiss, H.-G. Eckel, “Fundamental Frequency and Mission Profile Wearout of IGBT in DFIG Converters for Windpower”, 15th European Conference on Power Electronics and Applications (EPE), pp. 1-6, 2013

[2] K. Ma, M. Liserre, F. Blaabjerg, “Lifetime estimation for the power semiconductors considering mission profiles in wind power converter”, IEEE Energy Conversion Congress and Exposition, pp. 2962-2971, 2013

[3] G. Zhang, D. Zhou, F. Blaabjerg and J. Yang, “Mission profile resolution effects on lifetime estimation of doubly-fed induction generator power converter,” *2017 IEEE Southern Power Electronics Conference (SPEC)*, 2017

[4] T. Hunger, O. Schilling, “Numerical investigation on thermal crosstalk of silicon dies in high voltage IGBT modules”, PCIM Europe 2008

[5] A. Nieslony, Rainflow counting algorithm (v 1.2.0.0) available on MathWorks File Exchange, https://www.mathworks.com/matlabcentral/fileexchange/3026

[6] E. Cheynet, J. B. Jakobsen, C. Obhrai, “Spectral characteristics of surface-layer turbulence in the North Sea”, Energy Procedia, Volume 137, pp. 414-427, 2017

[7] B. Wu, Y. Lang, N. Zargari, et al., Power Conversion and Control of Wind Energy Systems, Wiley-IEEE Press, 2011.

[8] Y. C. Gerstenmaier, W. Kiffe and G. Wachutka, “Combination of thermal subsystems modeled by rapid circuit transformation,” *2007 13th International Workshop on Thermal Investigation of ICs and Systems (THERMINIC)*, 2007, pp. 115-120

[9] Infineon AG, “PC and TC Diagrams”, Infineon AG Application Note AN2019-05, Edition 2021-02-1919

[10] T. Methfessel, F. Sauerland, K. Mainka and O. Schilling, “Enhanced lifetime and power-cycling modelling for PrimePACK™ .XT power modules”, PCIM Europe digital days 2020, International Exhibition and Conference for Power Electronics, Intelligent Motion, Renewable Energy and Energy Management, 2020, pp. 1-8.

[11] T.-M. Plötz, J. Fuhrmann, H.-G. Eckel, „Powercycling Test Bench with Realistic Loss Distribution and Temperature Ripples“, 2022 24th European Conference on Power Electronics and Applications (EPE’22 ECCE Europe), 2022